FRICTION INDUCED VIBRATION

Wayne V Nack
Arun M Joshi

General Motors Corporation
Warren, MI 48090

ABSTRACT

Techniques have been developed to analyze friction induced vibration. A vehicle system model and the MSC/NASTRAN solutions for geometric nonlinear and complex modes were modified by DMAP for friction input. Both stable vibrations and unstable vibrations could be found with this method. To assess stability, a position of steady sliding equilibrium was found. Then a complex modes solution was done to find negatively damped modes. Mode shape animation of all the unstable modes showed that there was a 90° out of phase vibration. This produced a design modification on a test vehicle which stabilized the vibration and eliminated brake moan.

INTRODUCTION

A recent ASME Winter Annual meeting [1] devoted a section to friction induced vibration problems. A paper [2] in that conference presented a procedure for analyzing the dynamic stability of friction induced vibration problems and it is used in this study. If vibrations don't die out at damped steady state sliding ($t \rightarrow \infty$) , the response is defined to be dynamically unstable. Both linear and nonlinear systems use this definition. However, an unstable linear solution grows with out bound while the nonlinear solution produces a limit cycle oscillation of large amplitude. The onset of an instability is termed a bifurcation [6,7,10,11] since the solution changes character from a stable to an unstable one.

The following procedure will be used to assess stability. The response is first assumed to be stable and it is analyzed for any instabilities. If any instabilities are found, the design is changed until none remain. Then the first assumption is valid and the response is stabilized. If the response is stable and damping is present, then at ($t \rightarrow \infty$) the structural vibrations die out. This position will first show the onset of an instability in the system. A nonlinear transient solution can be run to find this position, but that is not necessary. If it is assumed that the friction law is not history dependent, then the stable sliding position can be found from statics. Complex eigenvalues are found in this position and if any root is in the right half root locus plane, an unstable solution is produced.

Nonlinear transient solutions [4] can also address dynamic stability problems. The nonlinear transient is repeatedly run by changing parameters in the system. When a large limit cycle oscillation of high amplitude is observed at steady state, the response is unstable. The nonlinearities constrain the system from growing with out bound, unlike a linear unstable solution. Many computer runs are required in this procedure and the concept of modes is lost. The amplitude of the periodic limit cycle can be found, but this is not needed as the linearized model can be used to avoid any unstable modes.

Previous work at General Motors included a study in reference [3] which was jointly done with SDRC. Several factors limited the usefulness of this work. There were numerical instabilities in the complex eigensolver in MSC/NASTRAN, circa 1985 that prevented an accurate stability evaluation. The investigators needed an animation method for complex modes so the out of phase motion could be verified for unstable modes. A more accurate distribution of the static pressure [13,18] between the brake pads and rotor may have been needed. The brake system was modeled as a rotor, pads, caliper and a flexibility constrained to ground. As all vehicle system parameters effect stability, more of the structure may have been needed and it may have been necessary to put the brake system into a vehicle system model.

A two step procedure was used in this study with MSC/NASTRAN for the stability analysis. A static solution, SOL 64 was run to find the steady sliding position ($t \rightarrow \infty$). Then the tangent stiffness matrix was input into a linearized complex modes solution, SOL 67. The modes with negative damping indicated instabilities. This procedure was reanalyzed repeatedly until a stable solution was found. This was used to predict the stability boundaries for different designs. It is exact

for responses in the stable region or at the onset of an instability. The response was stabilized by this method so a nonlinear transient solution was not needed.

PROBLEM AND MODEL

The problem analyzed was brake moan, but any other friction induced vibration problem could be addressed by the developed methods. Brake moan occurs at any vehicle speed > 2 mph. A middle frequency vibration in the 150 to 300 Hz range occurs during moan and the brake system and suspension vibrate strongly.

A full vehicle system model was employed in MSC/NASTRAN to study the phenomenon since it was determined that many suspension modes were excited. The body of the vehicle was assumed to be rigid with a mass and an inertia. The front and rear suspension were modeled as: rigids, beams, masses, springs, and dampers. The rubber parts used structural damping and the shock absorbers were modeled as viscous dampers. The tires were represented as modal properties. The engine was modeled as a rigid mass and inertia while the driveline was modeled as beams and springs.

It was experimentally determined that the rotor and caliper were moving as rigid bodies so the brake system consisted of a rigid rotor/caliper and experimentally measured spring rates for the mounting brackets, slider pins, etc. The brake system model is shown in figure 1. The center of pressure on the brake pads locates the effective resultant normal force due to the normal pressure distribution on the brake rotor surface. There is one CROD on the inboard and one on the outboard brake pad which represent the normal stiffness of the brake pad. To locate an approximate center of pressure, an inverse solution was done using observed global measurements on the vehicle system. An alternative method would measure the static pressure distribution [13,18] between the rotor and pads to locate the center of pressure. This may be necessary when the flexibility of the brake systen is important.

THEORY

A nonlinear transient run can be used to assess the stability of a dynamic motion. This can be described by the following state equations.

$$[M]\left\{\frac{\partial^2 u}{\partial t^2}\right\}+[C]\left\{\frac{\partial u}{\partial t}\right\}+[K_t(u)]\{u\}=\{P\} \tag{1}$$

$[M]$: Mass Matrix

$[C]$: Viscous damping matrix

$\{P\}$: Brake line pressure

$[K_t(u)]$: Tangent stiffness matrix

where the tangent stiffness matrix contains the linear structural stiffness matrix and it has nonlinearities due to : the brake line pressure as a preload; the friction stiffness; and the friction follower force [3,16]. After bifurcation, equation (1) gives a solution as a periodic limit cycle of large amplitude.

The objective of this study was to avoid any bifurcation and this was done by a two step procedure. The stable steady sliding (static) response occurs at $t \to \infty$. It can be used to predict the onset of an instability. The vibrational velocity and acceleration are zero in this position. Statics can then be used to predict this location if the friction law is not history dependent.

(2) $$\left[K(u^*) - \mu K_f(u^*)\right]\{u^*\} = \{P\}$$

[K] : preloaded tangent stiffness matrix

$[\mu K_f]$: friction stiffness

The tangent matrix $[K_t(u^*)]$ has been separated into a conservative part $[K(u^*)]$ due to the structural elements and a nonconservative part due to friction $-[\mu K_f(u^*)]$. The response in (1) is linearized about the steady sliding position, u^*. A dynamic perturbation is given to this position to determine stability.

(3) $$[M]\left\{\frac{\partial^2 u}{\partial t^2}\right\} + [C]\left\{\frac{\partial u}{\partial t}\right\} + [K_t(u^*)]\{u\} = \{0\}$$

By assuming a harmonic response in (3), a complex eigenvalue problem is formulated. This produces a linearized stability evaluation. It can be used to predict stable responses or those at the onset of a bifurcation.

(4) $$\{u\} = \{\phi\}e^{\lambda t}$$

(5) $$\left[\lambda^2 M + \lambda C_d + K(u^*) - \mu K_f(u^*)\right]\{\phi\} = \{0\}.$$

(6) $$\lambda = \alpha \pm i\omega$$

λ = eigenvalue

α = damping

ω = frequency

M = mass matrix

C_d = composite viscous damping

Friction is a nonconservative force, it dissipates energy out of the system, so the sign of the friction stiffness in equation (5) is negative. Since the brake rotor is rotating at a relative velocity that is larger than any vibrational velocity, the sign of the relative velocity is one way. The sign is not required in the friction stiffness of (5). Friction enters the complex eigenvalue problem (5) as both friction damping and friction stiffness as outlined below.

- Friction Damping

(7) $$F_f = C\left(\frac{\partial \Delta u_t}{\partial t}\right)$$

C = slope of friction vs velocity curve

$\frac{\partial \Delta u_t}{\partial t}$ = tangential relative velocity

- Friction Stiffness

(8) $$F_f = \mu N = \mu K_f \Delta u_n$$

K_f = normal stiffness between pad & rotor

μ = friction coefficient

Δu_n = relative normal displacement

The friction force deflection (8) is unsymmetric since a normal displacement, Δu_n induces a tangential force, F_f but not the reverse. This can be called a DC (direct current) frictional force and it enters (5) as an unsymmetric stiffness matrix to be described later.

A root locus diagram is presented in figure 2 for a varying parameter β in equations (2,5), where β can be anything defined in the model, i.e. stiffness, plate thickness, etc. The real axis is damping and the imaginary is frequency on this plot. For increasing β, two roots initially in the left half plane will eventually intersect at A which is called a limit point. For an additional change in β, the roots branch to the left and right half planes. Roots in the left half plane have positive damping and are stable, while those in the right half plane have negative damping and are unstable. When one root crosses the right half plane, a bifurcation [6,7,10,11] occurs since the system behavior changes due to an unstable solution being generated. Only nonconservative systems bifurcate and this is determined by the friction stiffness term. There is a smaller effect on bifurcation due to the coupling of the friction stiffness to the structure. The form of the limit point at A is determined by the unsymmetric friction stiffness matrix. It is called a flutter limit point in [6,7,11] since aeroelastic flutter shows the same type of behavior. For those interested in this, a more comprehensive treatment of limit points is found in Catastrophe theory [15]. The subject of Aeroelasticity [12] contains the same physics and mathematics as friction induced vibration, the only changes are between aerodynamic force and friction. The methods in this discipline can be converted for use in friction induced vibration problems.

For a small variation in β after bifurcation, the curved line C_1 - A - C_2 in figure 2 is symmetric. This means that the two modes C_1 , C_2 vibrate at the same frequency so they are coupled. The friction provides weak coupling between the two modes so they vibrate almost independently within a complex mode. Figure 3 shows two coupled modes where the coupling is weak due to the friction work. The modes in Figure 3 vibrate in the following pattern: S_1 is at max amplitude and S_2 is zero; later S_1 is zero while S_2 is at max amplitude. The time responses [5] for S_1 and S_2 show that the two are 90° out of phase. Sometimes the coupled modes are referred to as providing feedback: energy from one mode is fed into the other and visa versa. Energy is released per cycle when the strain energy becomes less than the frictional work. When this occurs, there is no stiffness left to restrain the system so energy is released out of the system in the form of kinetic energy. We will show in the design study that if the two modes can be decoupled, the bifurcation will be prevented and only a stable vibration will remain.

Physically on the vehicle, the braking operation sets up a stick slip vibration between the friction pads and rotor. Two possibilities can occur: the first is a stable vibration where the roots lie in the left half plane. This produces a resonance vibration behavior and is generally not a problem. The other case occurs when one or more roots cross into the right half plane. A bifurcation occurs which produces negative damping in the system.

MSC/NASTRAN IMPLEMENTATION

Within MSC/NASTRAN, a SOL 64 geometric nonlinear solution was initially made with the brake pressure applied as a steady sliding (static) preload. The friction stiffness was neglected in

equation (2) since the Newton iteration in version 67.5 MSC/NASTRAN did not allow for unsymmetric matrices. The tangent stiffness matrix was saved by DMAP and this was read into SOL 67, complex eigenvalue analysis. All of the matrices in SOL 67 were reduced by GDR (Ritz Vectors) prior to the Hessenberg complex eigenvalue extraction. As a result of current formulations in MSC/NASTRAN the complex eigensolvers can not mix both viscous and structural damping in one run. The result of this mixing produced a numerically unstable solution in version 67.5. To overcome this, the structural damping used on the rubber parts was converted to an equivalent viscous damping per mode, called composite damping. If KG is the modal structural damping matrix, and if weak damping/coupling is assumed then each row would be part of a modal equation. So the maximum viscous damping that would occur in each mode is the structural damping divided by the natural frequency for the mode in each row.

$$[C_d] = \begin{bmatrix} \frac{KG_{11}}{\omega_1} & \frac{KG_{12}}{\omega_1} & \cdots\cdots & \frac{KG_{1n}}{\omega_1} \\ \frac{KG_{21}}{\omega_2} & \frac{KG_{22}}{\omega_2} & \cdots\cdots & \frac{KG_{2n}}{\omega_2} \\ \cdot & \cdot & \cdot & \cdot \\ \frac{KG_{n1}}{\omega_n} & \frac{KG_{n2}}{\omega_n} & \cdots\cdots & \frac{KG_{nn}}{\omega_n} \end{bmatrix} \tag{9}$$

The composite damping was implemented in a SOL 67 complex modes solution by a special DMAP program. The effect of the composite damping was to smear the structural damping out to every mode as viscous damping. It was a good approximation for a vehicle since the viscous shock absorber damping was larger than the structural dampers on the rubber parts. The slope of the friction vs relative velocity curve was accounted for by using the CDAMP2 dampers between the sliding contact grid points on each surface as shown in Figure 4. The friction stiffness was implemented on DMIG cards as shown in figure 5 for the two coincident nodes 100 and 200 which were on the rotor and caliper. The friction force is converted into the coefficient multilpied by the normal stiffness and relative normal displacement. The normal stiffness between the two nodes is K_f in figure 5 and it represents the flexibility of the brake pads.

RESULTS

Using experimental modal analysis, the following motion was observed within the complex mode at the brake moan frequency: torque arm bending, cross car brace bending, lower control arm bending, rear axle tube torsion, rear axle tube bending, and axle shaft bending. The real time animation (FFT shapes) measurements during moan showed the following: rigid body rotational ϕ, and translational θ, motion of the caliper with respect to the rotor as shown in figure 6. The rotor was not instrumented since it rotates during moan and it is a difficult measurement to take.

Because of this it was not possible to see any friction motion during this test. The experimental complex modal analysis did not show any friction motion since the curve fitting routines are for conservative systems only. So it was not possible to see any friction motion in the complex mode from test and it was also not possible to see any coupled modes due to friction.

The finite element solution showed a complex mode with negative damping and a frequency within 7% of experimental data during brake moan. The component motion within this mode correlated visually with experimental data. Additionally, the finite element model showed friction motion in the complex mode which was unavailable in the experimental modal analysis. Animation of the complex modes was done by the INSTANT program which properly showed a phase variation in the structural mode between grid points. The animated complex mode showed a motion due to friction which was not available from test. Referring to figure 6, the friction motion showed a relative rotational motion, $\Delta\phi$ of the caliper with respect to the modal deformed position of the rotor. This relative motion, $\Delta\phi$ was such that the caliper and rotor vibrated 90° out of phase in the unstable complex mode during brake moan. A translational motion, θ of the caliper with respect to the rotor was also shown. The friction also caused coupling between the bending of the axle shaft and bending of the axle tube. Without friction, these modes were 2 Hz apart in frequency and they became coupled due to the friction. It was concluded that good correlation was made between the analytical and experimental measurements.

Several changes had a small effect on stability for this problem only. Friction damping had a negligible effect on stability. By changing the friction coefficient in the normal operating range of .3 to .4 , stability could not be achieved.

Several design alternatives were evaluated to stabilize the motion. The key was to remove the 90° out of phase motion , $\Delta\phi$ of the caliper relative to the rotor. A design proposal was developed which stabilized the motion by decoupling the axle tube bending from the axle shaft bending. This eliminated the 90° out of phase motion, $\Delta\phi$ between the caliper and rotor. This design proposal was evaluated in hardware on a test vehicle and it performed as predicted by the simulation; brake moan was eliminated.

EXTENSIONS

Good results were obtained with the above formulation, but the following extensions may be required to analyze other types of friction induced vibration phenomenon. Equation (8) is the standard form of Coulomb's friction law where the friction coefficient is a constant independent of normal force, N. For dynamic friction in a vibration problem, there is evidence [8,9] that μ varies with N. So the inclusion of a linear variation of μ with respect to N is presented,

$$F_f = (\mu + DN)N = \mu K_f \Delta u_n + D K_f^2 \Delta u_n^2$$

where μ is the intercept and D is the slope of the μ vs N curve. The friction force can be expanded as a first order Taylor series to give the linearized form.

$$(10) \qquad F_f = (\mu K_f + 2DK_f^2 \Delta u_n^*)\Delta u_n$$

If the measurement of the constant D were made, (10) could be formulated, where Δu_n^* is the normal deflection due to the steady sliding preload.

This study did not consider friction to be a follower force as discussed in reference [16]. For completeness, Figure 7 presents two bodies with friction on the interface surface. The friction force remains tangent to the interface and rotates with the bodies. A vertical force is picked up at the nodes due to this rotation. These forces are shown in Figure 7 and are projected onto the vertical direction by the angle, ϕ. A force deflection relation, [A] is shown in Figure 8 where the stiffness coefficients are found by differentiation,

$$(11) \qquad K_{ij} = \frac{\partial F_i}{\partial u_j}$$

The nonlinear solution in MSC/NASTRAN needs to be modified to account for displacement dependent terms in [A] as well as equation (10). A module can be added to a user modifiable version of MSC/NASTRAN that would form the matrix [A] of Figure 8 and equation (10). Then the displacement dependent terms could be updated each time inside the nonlinear loop for every load increment.

CONCLUSIONS

These techniques can be used to understand the physics of friction induced vibration. Stability was analyzed by linearizing the equations about steady sliding and a complex modes analysis was done to examine stability. Those modes with negative damping were unstable and showed a 90° out of phase motion. They were stabilized with the developed method and this produced a vehicle design that eliminated brake moan.

Other types of friction induced vibration problems may be analyzed with this method like brake squeal, brake grunt, etc. Brake squeal occurs at any vehicle speed when a high pitched noise in the 2 to 20 Khz range is produced. Brake grunt occurs at a slow creeping speed, < 2 mph when a low frequency grinding noise is produced. It may be necessary to add the indicated extensions in this paper to MSC/NASTRAN for these problems.

REFERENCES

1.Ibrahim,R.A., Soom,A. (eds.), *Friction Induced Vibration, Chatter, Squeal and Chaos,* ASME DE - VOL 49, 1992.

2.Tworzydlo,W.,W., Oden,J.T., et al, "Numerical Modeling of Friction Induced Vibrations and-Dynamic Instability", ASME DE - VOL 49, 1992.

3.Liles,G.D., "Analysis of Brake Squeal Using Finite Element Methods", SAE paper 891150, 1989.

4.Kikuchi,N., Oden,J.T., *Contact Problems in Elasticity: A Study of Variational Inequalities and Finite Element Methods* , SIAM , 1988.

5.Marion,J.B., Thornton,S.T., *Classical Dynamics of Particles and Systems,* 3rd edition, Harcourt, Brace, Jovanovich, 1988.

6.Huseyin,K., *Vibrations and Stability of Multiple Parameter Systems,* Sijthoff & Noordhoff, 1978.

7.Ziegler,H., *Principles of Structural Stability,* Blaisdell, 1968.

8.Rhee,S.K., "Friction Coefficient of Automotive Friction Materials - Sensitivity to Load, (Normal Force), Speed, Temperature", SAE paper 740415, 1974.

9.Srinivasan,A.V., "Dynamic Friction" in *Large Space Structures Dynamics and Control,* Springer, 1988.

10.Seydel,R., *Practical Bifurcation and Stability Analysis : From Equilibrium to Chaos,* Springer Verlag , 1994.

11.Huseyin,K., *Multiple Parameter Stability Theory and its Applications: Bifurcations, Catastrophes,* Instabilities, Oxford , 1986.

12.Dowell,E.H., et al , *A Modern Course in Aeroelasticity* , Kluwer, 1989.

13.Samie,F., Sheridan,D., "Disc Brake Rotor/Pad Contact Analysis with Friction", SAE paper 900005, 1990.

14.Leipholz,H., *Stability Theory: An Introduction* , Wiley , 1987.

15.Gilmore,R., *Catastrophe Theory for Scientists and Engineers,* Wiley , 1981.

16.Mottershead,J.E., Chen,S.N., "Brake Squeal - An Analysis of Symmetry and Flutter Instability", ASME DE - VOL 49, 1992.

17.Bremner, P.G., "Finite Element Basis for Understanding Chatter and Squeal Instabilities", Melbourne, 19 - 21 , August 1987.

18.Kao,T.K.,Richmond,J.W.,Moore,M.W.,"The Application of Predictive Techniques to Study Thermo Elastic Instability of Brakes", SAE paper 942087, 1994.

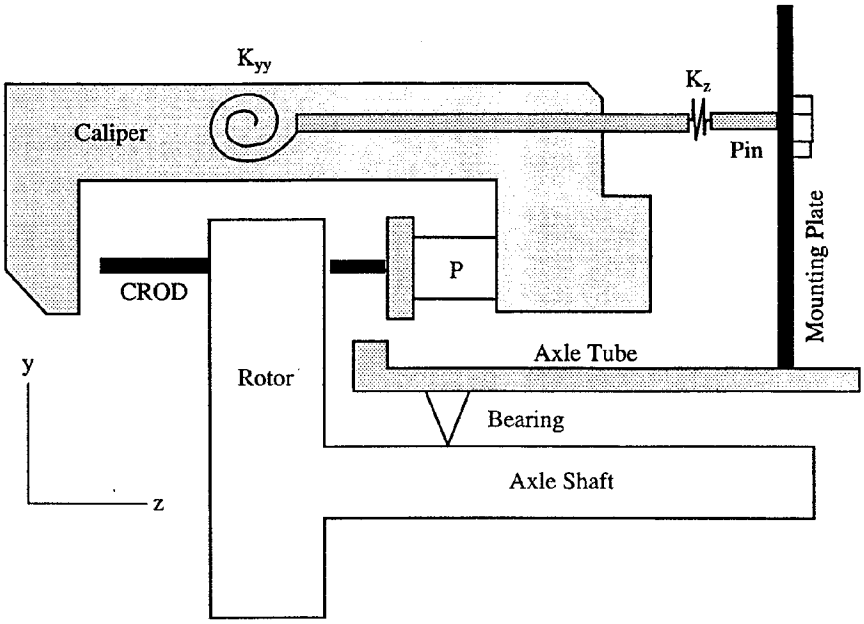

Caliper:	Rigid
Rotor:	Rigid
Mounting Plate:	Rigid
Axle Tube:	Beams
Axle Shafts:	Beams
CROD K_f:	Model of Brake Pad (Experimentally Measured Stiffness)

K_{yy}: Torsion Stiffness Mounted Caliper (Experimental)
K_z: Friction Stiffness Pins (Experimental)

BRAKE SYSTEM
Figure 1.

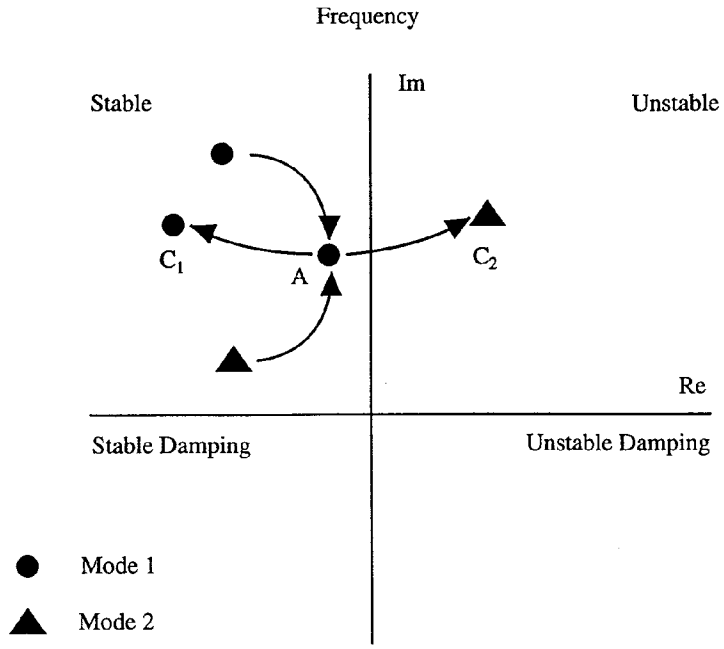

ROOT LOCUS PLOT
INCREASING PARAMETER β
Figure 2.

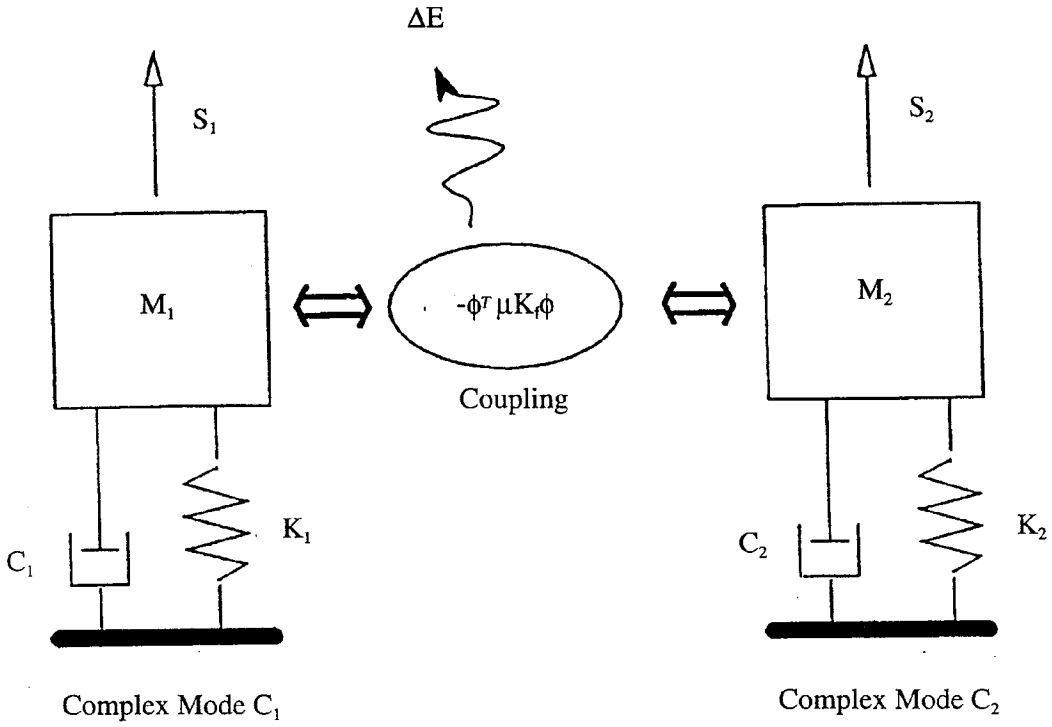

AFTER BIFURCATION
WEAKLY COUPLED MODES
Figure 3.

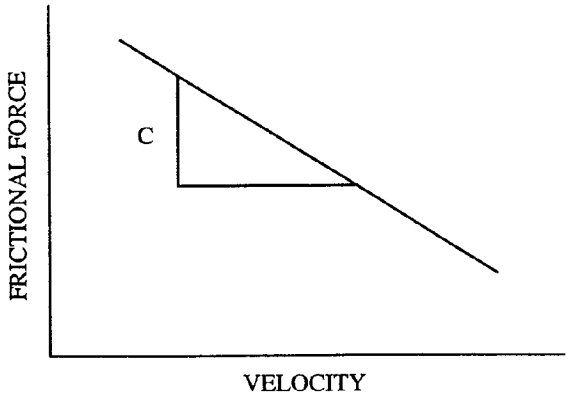

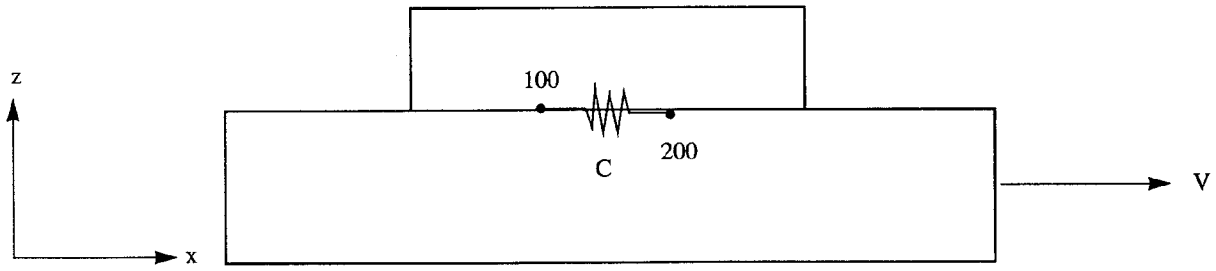

$$F_{200,1} = C\,[\dot{u}_{200,1} - \dot{u}_{100,1}]$$
$$F_{100,1} = C\,[\dot{u}_{100,1} - \dot{u}_{200,1}]$$

FRICTION DAMPING
CDAMP2 CARD INPUT
Figure 4.

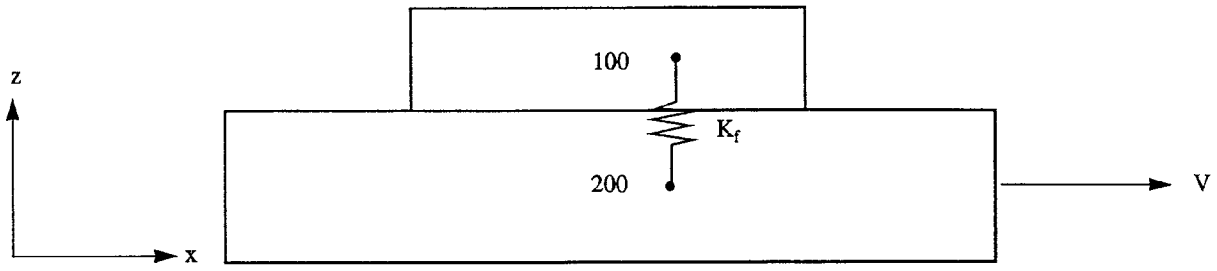

$$F_{100,1} = -\mu.K_f\,[u_{100,3} - u_{200,3}]$$
$$F_{200,1} = -\mu.K_f\,[u_{200,3} - u_{100,3}]$$

$[\mu.K_f] =$

	100,3	200,3
100,1	$-\mu.K_f$	$+\mu.K_f$
200,1	$+\mu.K_f$	$-\mu.K_f$

FRICTION STIFFNESS
DMIG CARD INPUT
Figure 5.

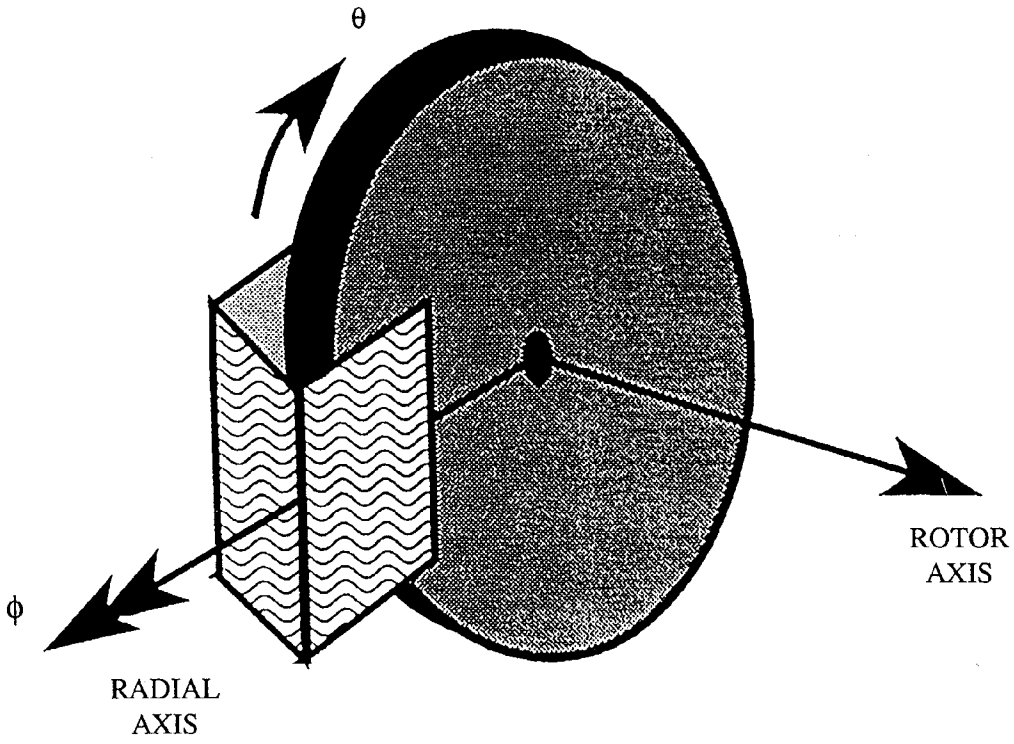

CALIPER ROTOR FRICTION MOTION
Figure 6.

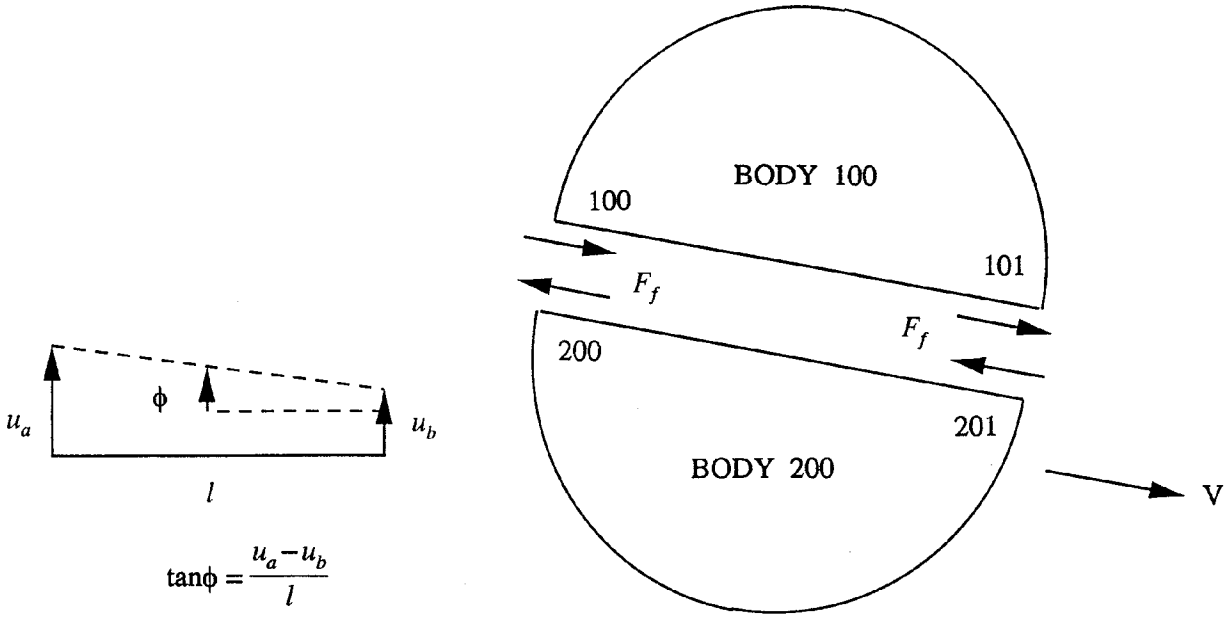

$$F_{200,3} = (\frac{u_{200,3} - u_{201,3}}{l})\mu K_f(u_{100,3} - u_{200,3})$$

$$F_{201,3} = (\frac{u_{200,3} - u_{201,3}}{l})\mu K_f(u_{101,3} - u_{201,3})$$

$$F_{100,3} = (\frac{u_{100,3} - u_{101,3}}{l})\mu K_f(u_{100,3} - u_{200,3})$$

$$F_{101,3} = (\frac{u_{100,3} - u_{101,3}}{l})\mu K_f(u_{101,3} - u_{201,3})$$

Friction Follower Forces
Figure 7

$$
\begin{array}{c}
\\
\frac{\mu K_f}{l}
\end{array}
\begin{array}{c}
\begin{array}{cccc}
u_{100,3} & u_{200,3} & u_{101,3} & u_{201,3}
\end{array} \\
\begin{bmatrix}
2u_{100,3}-u_{200,3}-u_{101,3} & -u_{100,3}+u_{101,3} & -u_{100,3}+u_{200,3} & \mathrm{O} \\
u_{200,3}-u_{201,3} & u_{100,3}-2u_{200,3}+u_{201,3} & \mathrm{O} & -u_{100,3}+u_{200,3} \\
u_{101,3}-u_{201,3} & \mathrm{O} & u_{100,3}-2u_{101,3}+u_{201,3} & -u_{100,3}+u_{101,3} \\
\mathrm{O} & u_{101,3}-u_{201,3} & u_{200,3}-u_{201,3} & -u_{200,3}-u_{101,3}+2u_{201,3}
\end{bmatrix}
\end{array}
\begin{array}{c}
\\
\begin{array}{c}
F_{100,3} \\ F_{200,3} \\ F_{101,3} \\ F_{201,3}
\end{array}
\end{array}
$$

Friction Follower Matrix [A]
Figure 8